# Electrical resistivity, wettability, and structural properties of oriented columnar Mo thin films

**Khaoula RAHMOUNI[a,b], Ilyas BENSALEM [c] , Abdelhamid BENHAYA[d], Nicolas MARTIN[e]**

[a] Laboratory of Active Components and Materials. Larbi Ben M'hidi University Oum El Bouaghi. BP 04000, Algeria.

[b] ISTA, University of Larbi Ben M′hidi, Oum El Bouaghi, Algeria

[c] Mechanics of Structures and Materials Laboratory,University of Batna 2, Batna, Algeria.

[d] Laboratory of Advanced Electronics, Department of Electronics, University of Chahid Mostefa Benboulaid Batna 2, Batna, Algeria

[e] Institut FEMTO-ST, SUPMICROTECH-ENSMM, CNRS, 15B, Avenue des Montboucons, 25030, Besançon Cedex, France

**Abstract:**

This work reports on the effects of Oblique Angle Deposition (OAD) on the microstructure, electrical resistivity, and wettability of molybdenum (Mo) thin films. DC magnetron sputtering is used to deposit Mo on silicon wafers while the substrate inclination angle is varied from $\alpha$ = 10° to 80°. Thin film crystalline structure is analyzed by X-ray diffraction and shows that for a substrate inclination angle lower than 60°, the (110) peak of the bcc Mo phase becomes more pronounced. Using the contact angle technique, it is found that Mo films are hydrophobic with an improved wettability as $\alpha$ angle tends to be glancing. Results indicate that rather than adjusting the composition of thin films, it is possible to affect their properties by modifying their nanostructured design. Morphological characteristics of Mo thin films show a significant voided architecture as the substrate inclination angle rises. An oxygen enrichment is also obtained, and Mo films become less conductive with an electrical resistivity increasing by two orders of magnitude as the substrate inclination angle reaches 80°.

**Keywords:**

Mo thin films, OAD, DC magnetron sputtering, Electrical resistivity, Wettability.

**Graphical abstract**

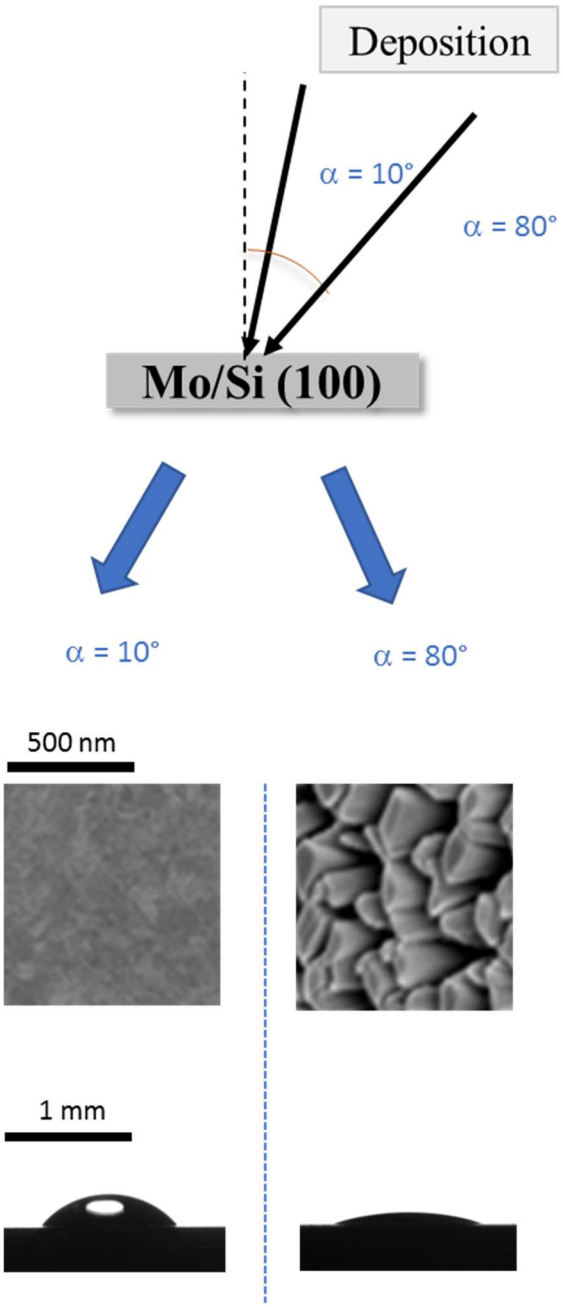

**Highlights**

- Mo thin films were deposited by OAD PVD.

- Columnar architecture can affect chemical composition and electrical resistivity.

- The highest substrate inclination angle produces significantly enhanced wettability.

- The properties of Mo films are linked to the flow inclination angle and the architecture of the films.

## 1. Introduction

Since characteristics of molybdenum and similar compounds greatly depend on the oxidation state of the metal [1], they have found extensive uses in industry. Inorganic molybdenum compounds, such as metallic molybdenum, $MoN_x$, $MoO_3$, and $MoS_2$, are now involved in a variety of fields, including gas sensing, energy storage, field emission, photo- and electro-chromic devices, and hole transport layers for photovoltaics, because of the multiple accessible molybdenum oxidation states and the potential changes in their crystal structures upon excitation by light, heat, or applied voltage [2, 3]. They have also been the focus of many studies in the disciplines of coordination, bioinorganic, cluster, solid-state materials, organometallics/catalysis, and solid-state materials [4-7]. Metallic molybdenum and its oxides, nitrides, and sulphides have recently gained interest as cutting-edge materials in electronic and semi-conductor research [8, 9]. Thin films with thicknesses measured in the Angström to nanometer range are among the many structural forms of these compounds, and they are particularly significant in the current and upcoming microelectronic and display industries. Gas-phase deposition techniques, including physical vapor deposition (PVD) and chemical vapor deposition (CVD), have been widely researched as a generic technique for producing thin films [10, 11]. Although thin films deposited by PVD have limited step coverage, they benefit from very low impurity levels and superior film quality.

A wide variety of materials can be used to create nanoporous structures using additive or subtractive processes that involve surface deposition, such as pulsed laser deposition, chemical or physical vapor deposition, or sol-gel [12]. Subtractive processes based on material etching, such as chemical, electrochemical, and e-beam, can also be used to create nanoporous structures. Oblique Angle Deposition (OAD), a physical vapor deposition technique for thin films with the substrate tilted, is one of them. Such a technique became increasingly important because it is a scalable and environmentally friendly fabrication method that works with a variety of materials and enables the creation of various nanostructured morphologies. Since the middle of the 20th century, OAD has been an original method for creating porous morphologies [13, 14]. Today, OAD is becoming a widely used method for depositing nanocolumnar thin films with nanoporosity for numerous applications, providing simple control over the morphology and porosity of the thin films by simply adjusting the deposition parameters. OAD significantly increases the thin film's porosity by taking advantage of the shadowing effect brought on by increasing columns when the substrate is tilted [12]. The tilt angle affects the shadowing effect, which in turn affects the size of pores and columns. According to earlier

reports [15, 16], isolated columns begin to develop with an increase in pore size. Other factors, including deposition time (film thickness) [17], deposition rate [18], deposition pressure [19], and gas composition [20], may also have an impact on the morphology of thin films formed by OAD, although there is not always a direct correlation between all these experimental conditions [21].

This work seeks to synthesize Mo films by magnetron sputtering utilizing the OAD method onto silicon substrates because there is a lack of thorough understanding regarding the characteristics of Mo films as a function of the substrate inclination angle. As this angle changes during deposition from 10° to 80°, surface morphology, microstructure, electrical characteristics, crystalline structure, and wettability of Mo films are investigated and discussed.

## 2. Experimental part

### 2.1 Surface preparation

All (100) silicon substrate rectangle pieces (side length of 15 mm, width of 10 mm, and thickness of 0.38 mm) were ultrasonically cleaned by a 15-minute sequential sonication process in acetone, then rinsed with ethanol, dried, and stored at room temperature. Then, Mo thin films were deposited by DC magnetron sputtering with a circular (51 mm in diameter) Mo metallic target (purity 99.99 at. %). Our experimental facility used to deposit the proposed structure was a homemade sputtering chamber pumped down by means of a primary pump followed by a turbo-molecular pump, enabling a residual vacuum pressure of $10^{-6}$ Pa. The sputtering process was carried out in an argon atmosphere at a sputtering pressure of 0.30 Pa with an inlet of 2.6 sccm of pure argon. The DC power supply was used to ignite plasma in the chamber, providing a constant current of 200 mA and a resulting Mo target voltage $U_{Mo}$ = 295-300 V. Besides, the substrate/Mo target distance was kept at 6.5 cm. The deposition process of the Mo architectures was carried out at room temperature and the deposition time was adjusted to obtain similar thickness for each sample (thickness of 800 nm). The OAD technique was used to grow Mo thin layers with oriented column's structure. The main idea behind this method resides in utilizing an oblique incident flux of the sputtered particles to deposit thin films tilting the substrate holder with a given angle, namely the substrate inclination angle $\alpha$. To assess the influence of the obliquely columnar structure Mo top film on the morphology, electrical resistivity, wettability and structure performances, various substrate inclination angles $\alpha$ = 10, 40, 60, and 80° were considered.

### 2.2 Thin films characterization

Scanning Electron Microscopy (SEM), which makes use of the JEOL JSM 7600F to observe the surface morphology and cross sections of the deposited films, was used to assess the morphological properties of the analyzed Mo films with an inclined structure. Using the same SEM running at 5 kV, the energy dispersive X-ray spectroscopy (EDS) was utilized to ascertain the produced sample's elemental chemical. Crystalline structure was analyzed with a Panalytical Aeris diffractometer with a copper X-ray tube (Cu $\lambda_{K\alpha 1,2}$ = 0.15418 nm) with a grazing incidence configuration at a constant angle θ = 0.8°. Scans were performed with a 2θ angle ranging from 35° to 90° with a step of 0.0204° per 1 s. The four-point probing approach developed by van der Pauw was used to assess the room temperature electrical characteristics of the OAD Mo films [22] using a Hall Measurement System Ecopia HMS5500 .

The wettability and the free surface energy (SFE) $\gamma_L$ of Mo films deposited at different angles (α = 10, 40, 60, and 80°) were determined from measurements of the contact angle ε. Four liquids of different polar ($\gamma_L^p$) and dispersive ($\gamma_L^d$) components (Table 1): distilled water, diiodo-methane, ethylene glycol, and glycerol were employed for measuring the contact angle with a device ramé-hart Model 790. The contact angles ε were obtained in ambient air using the standing drop method.

**Table 1.** Parameters of probe liquids used in evaluating surface free energy $\gamma_L$ (SFE) from contact angle ε (CA) measurements. $\gamma_L{}^d$ and $\gamma_L{}^p$ are the dispersive and polar component of the surface free energy: $\gamma_L = \gamma_L{}^d + \gamma_L{}^p$, respectively.

| **Liquids** | **Surface free energy $\gamma_L$ (mJ/m$^2$)** | **Dispersive component $\gamma_L^p$ (mJ/m$^2$)** | **Polar component $\gamma_L^d$ (mJ/m$^2$)** |
|---|---|---|---|
| Distilled water | 72.8 | 51 | 21.8 |
| Diiodo-methane | 50.8 | 0 | 50.8 |
| Ethylene glycol | 48 | 29 | 19 |
| Glycerol | 64.0 | 34.0 | 30.0 |

The wetting liquid was distributed over the surface of the sample to be characterized by a micrometric syringe using a dosing unit controlled by a motor and the image of the drop was recorded. A volume of 5 µl was used for the four liquids. The average value of the contact angle

(average of the left and right angles of each drop) was calculated after 180 seconds, taken at three different locations on the sample surface. The surface free energy of each film was calculated from the contact angle using the theory of Owens, Wendt, Rabel, and Kaelble (OWRK) [23-25].

## 3. Results and discussion

### 3.1 Cross-sectional and surface analysis:

Figure 1 displays, for the Mo films with the sputter-deposited structure created using the OAD process, the SEM cross-section and surface morphology images at α = 10, 40, 60, and 80°.

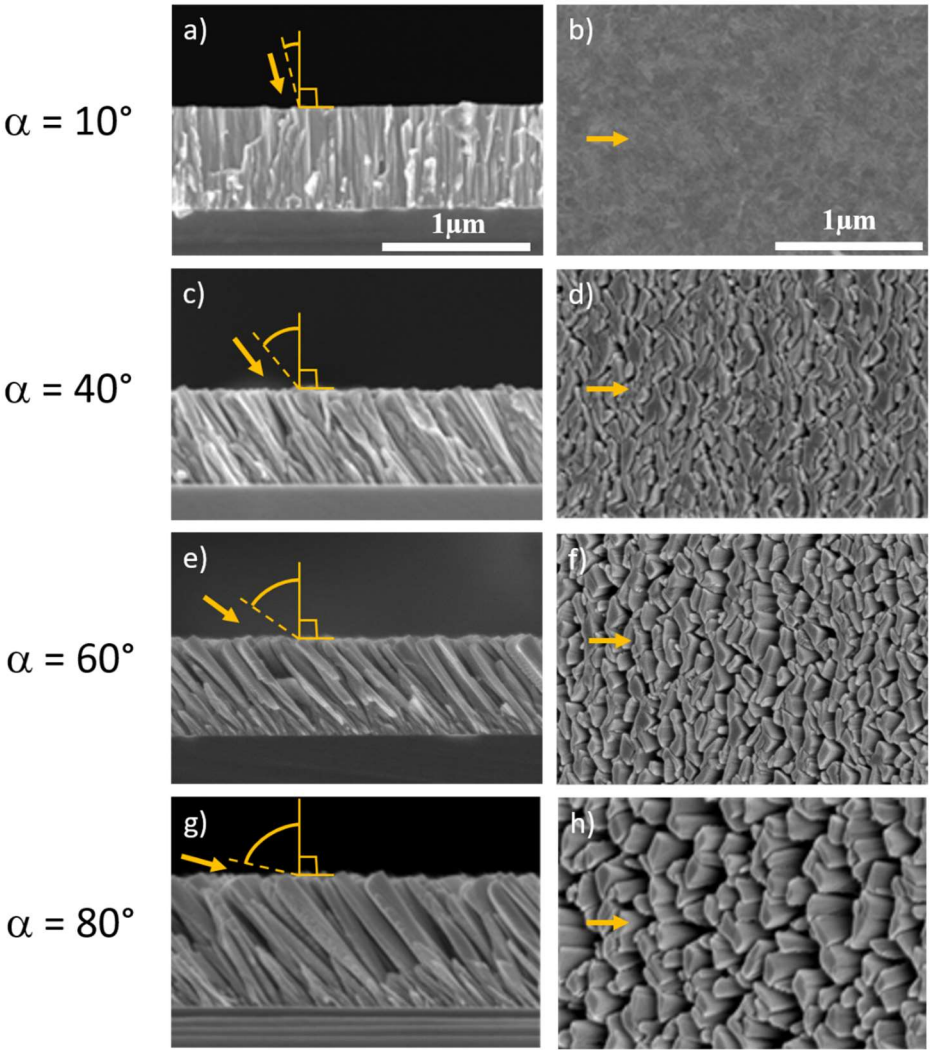


**Fig. 1.** SEM images of cross-sections and surface morphologies of the sputter-deposited Mo thin films prepared by OAD with substrate inclination angles of α = 10, 40, 60 and 80°. The incoming particle flux is indicated with arrows.

The surface morphology of the thin films created using the oblique deposition procedure shows inter-columnar porosity in conjunction with surface roughness morphology. Randomly spaced columns that are relatively related to another one are visible from the top view of the inclined Mo thin films. The surface dispersion of sputtered particles and the restricted shadowing mechanism are primarily responsible for these morphological characteristics. In essence, self-shadowing film deposition and subsequent formation of a porous, thin film with a columnar structure result from the development of the obliquely oriented Mo film on the Si substrate, which is inclined at $\alpha$ = 10, 40, 60, and 80°. While using the OAD technique at oblique angles of 40, 60°, and 80° results in regular and visible inclined rods that favor the direction of the incident particle flux with a column angle $\beta$ (angle between the normal to the substrate surface and the columns direction). An average of five values was then measured for each oblique angle leading to $\beta$ = 31°, 38°, and 41°, respectively (from SEM cross-section views in Fig. 1). Figure 2 compares the evolution of experimental column tilt angles of Mo films *vs.* substrate inclination angle $\alpha$ with the two geometrical models: tangent rule [26] and Tait's rule [27].

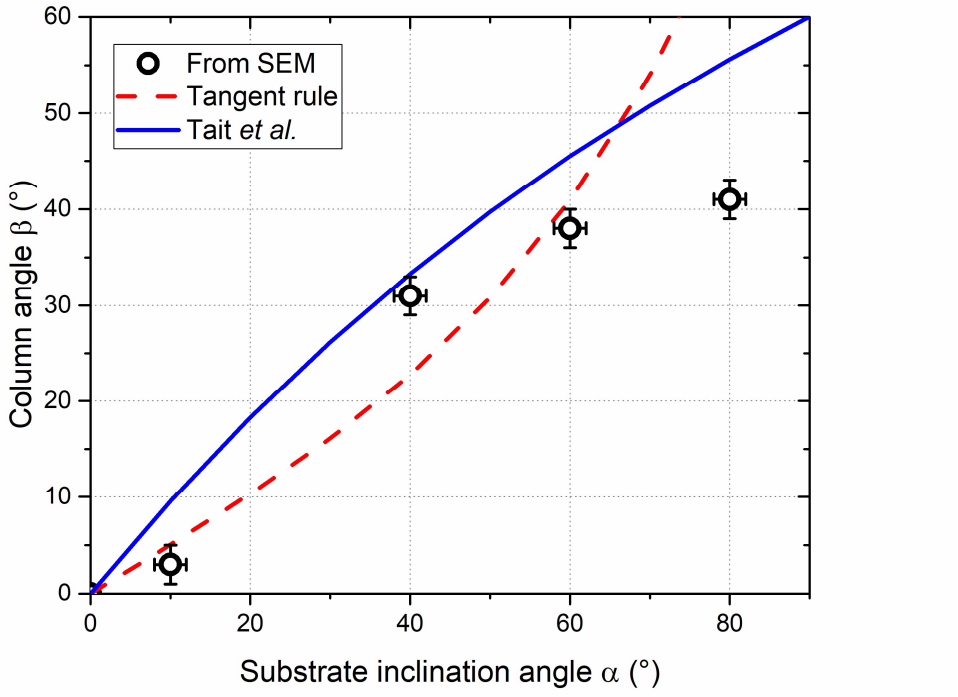


**Fig. 2.** Column tilt angle $\beta$ as a function of the substrate inclination angle $\alpha$ of Mo films. Tangent rule and Tait's rule are compared to the experimental column angles obtained from SEM observations for Mo films prepared with $\alpha$ = 10, 40, 60 and 80°.

It is noteworthy that the tangent rule is not suitable for substrate inclination angles higher than 50° [28]. The second model proposed by Tait *et al.* [29] is a purely geometrical relation that is derived from a ballistic model. According to Tait's rule, this implies that the column angle rises as a function of the substrate inclination angle. None of the geometrical rules are followed by our Mo films. In particular, it has been reported that it depends on the type of material deposited and deposition conditions [21, 30-32]. It is also worth noting that the particle flux generated by the sputtering of a target in a plasma is characterized by a relatively spread angular distribution. As a result, particles impinge on the substrate and the growing film with various angles of incidence and above all, different from the substrate inclination angle $\alpha$. Thus, it is not the geometric substrate inclination angle but the angle of incidence of the atoms that dictates, by shadowing effect, the inclination of the columns. Laterally spaced columns are created and placed along the growth. This is most likely because there isn't any atomic shadowing perpendicular to the growth plane, which results in a second structural anisotropy and allows the development of inclined columnar architecture [33]. It is also interesting to note that such obtained morphological properties have been demonstrated in several prior investigations, where inclined structures may be created by optimizing the deposition parameters of the OAD approach [34-38].

### 3.2 Crystallographic analysis and chemical composition

To learn more about the crystallographic structure evolution as a function of the substrate inclination angle, GIXRD investigations of Mo thin films are conducted (Fig. 3). For all samples, the pattern consists of a peak at $2\theta$ about 40.5° assigned to (110) planes of pure body-centered cubic (bcc) Mo phase. For $\alpha < 60°$, thin films show one strong and two somewhat faint diffraction peaks. The three diffraction peaks marked by Mo in the pattern can be identified as the (110), (200), and (211) crystal planes of the bcc structure. However, thin films deposit at $\alpha \geq 60°$ exhibit a low (110) diffracted signal when the substrate inclination angle rises. (Fig. 3b). This is expected for bcc lattices such as Mo because of the minimum surface energy linked to the very dense packing (110) planes [18]. This orientation has also been reported and can be attributed to the preferred directions intrinsic to evaporation or sputtering processes [19, 20]. The (110) peak exhibits a non-monotonic intensity fluctuation increasing the substrate inclination angle $\alpha$, as seen in Fig. 3b. When Mo film is deposited at $\alpha = 10°$, the (110) intensity is at its highest. The larger width is connected to the reduction of the grain size and change of

microstrain in the film. Lattice constant and crystal size were calculated using Scherrer's formula (Table 2).

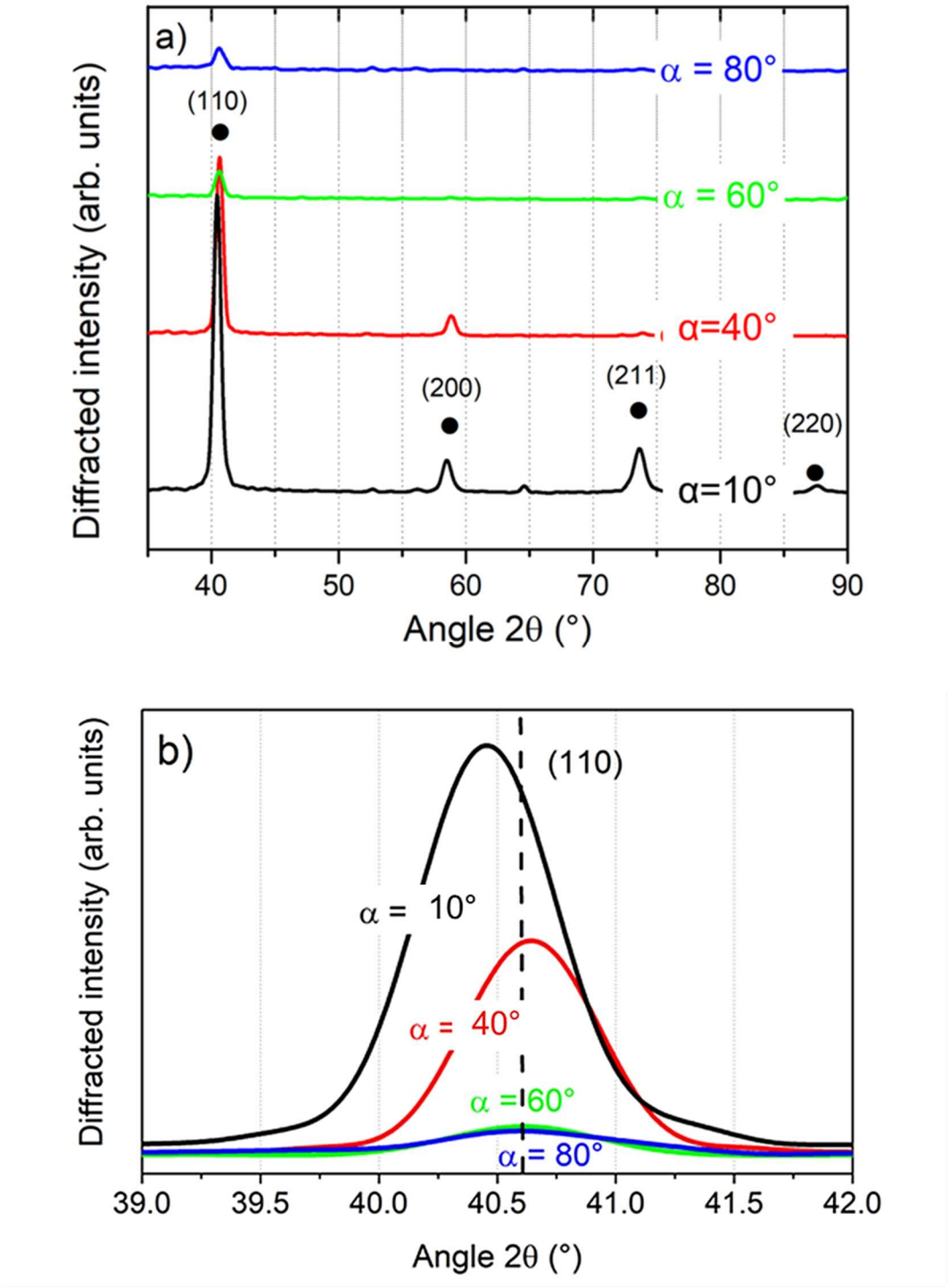


**Fig. 3:** a) GIXRD patterns Mo thin films 800 nm thick sputter-deposited on silicon for 4 different substrate inclination angles α. b) Focus on the diffracted signal corresponding to the (110) planes of the bcc Mo structure (the dotted line indicates the theoretical position).

Grain-size remains nearly unchanged and close to 12 nm for Mo films sputter-deposited for the lowest angles ($\alpha < 60°$) then diminishes to 8.9 nm for the highest one $\alpha = 80°$. This decrease is typically observed in GLAD films as the deposition angle tends to grazing incidence and higher than a critical angle (i.e., $\alpha > 60°$) [30]. This reduced long-range order is mainly assigned to the decrease of energy per deposited particle as the substrate inclination angle rises [19, 26]. The amount of thermalized sputtered particles prevails overs the ballistic species leading to less energetic deposited Mo atoms impinging on the growing film. In addition, shadowing effect predominates for the highest substrate inclination angles, which also correlates with a smaller crystal size and the loss of a preferential orientation.

**Table 2.** Lattice constant and crystal size from Scherrer's formula of Mo thin films prepared with different substrate inclination angles.

| Substrate inclination angle α (°) | 10 | 30 | 60 | 80 |
|---|---|---|---|---|
| Lattice constant a (± 0.005 Å) | 3.149 | 3.135 | 3.138 | 3.139 |
| Crystal size L (± 0.5 nm) | 12.4 | 12.6 | 11.1 | 8.9 |

Deposition at grazing angles also favors a voided columnar architecture and so, high films porosity (more than 50% of voids in some GLAD films [39]). As a result, impurities intrinsic to the vacuum process (mainly residual water vapor and oxygen species, as it will be shown later in § 3.3) disturb the crystalline growth in the columnar structure and so, it also contributes to the deposition of poorly crystallized films.

For the lowest substrate inclination angle $\alpha = 10°$, the lattice constant a = 3.149 Å, which is very close to the stress-free lattice parameter $a_{bulk}$ =3.147 Å [40]. An increase of α from 30 to 80° shifts the (110) diffracted signal to higher 2θ angles. This corresponds to a slight reduction of the lattice constant but it remains around the bulk value. These results agree with former investigations published by Abadias *et al.* [41] who also reported significant evolutions of crystal structure (preferential orientation, lattice constant, stress) for substrate inclination angle α higher than 35°. We may likewise assume that increasing α favors to the development of tilted columns with a more voided architecture. It is assigned to the shadowing effect and a decrease of average energy per deposited particle when α rises. These results also suggest a stress relaxation phenomenon for substrate inclination angle α higher than 30°, as it has ever been observed in GLAD films. According to Grigoriev *et al.*, [42], voids between the tilted columns absorb stresses arising in the film due to deposited high-energy atoms. Absolute values

of the stress decrease as the film thickness is higher than 10-20 nm (order of magnitude when shadowing effect starts to be significant) and the stress sign can also be changed with the growth (from compressive to tensile).

For determining the chemical composition of the Mo thin films, EDX microstudies were carried out as a function of the substrate inclination angle, especially the Mo and O atomic concentrations (Fig. 4).

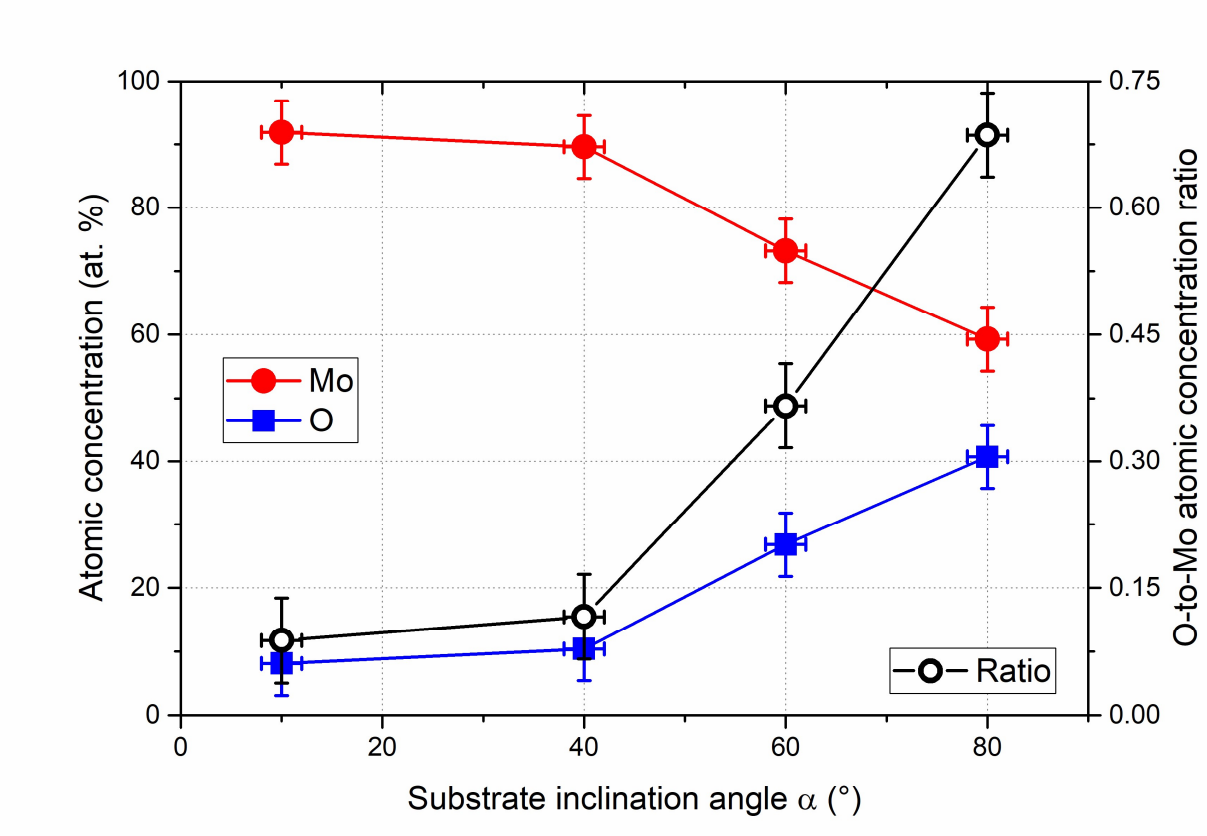


**Fig. 4.** Oxygen and molybdenum atomic concentrations, and oxygen-to-molybdenum concentration ratio in the sputtered Mo thin-films as a function of the substrate inclination angle α.

The presence of porosity in the layer permits and promotes the oxygen incorporation due to the residual atmosphere of the sputtering process and from the air when samples are put at atmospheric pressure. As the substrate inclination angle increases, the oxygen concentration in Mo thin films steadily rises. Tilting the substrate more and more favors the shadowing effect and leads to better separated columns. It also enhances the surface roughness producing a larger contact surface with oxygen from the air [43–45]. There are two potential sources of oxygen: (i) Oxygen adsorption on the surface of the thin films and forms an oxide. It is then mainly

located at the surface level, in voids created by the inter-columnar architecture. (ii) Secondly, during the deposition process, oxygen is trapped in the chamber. This type of oxygen is part of the chemical composition of the layer [46]. Indeed, in this study, the oxygen content in the films is in the 10–40 at % range. These values are significantly larger compared to the amount (7–8 at. %) found in the reference and fully-dense Mo film deposited at $\alpha = 10°$, suggesting that the presence of oxygen for the OAD Mo film series deposited at ambient temperature is primarily due to post-growth contamination in ambient air. An increased film porosity is expected to result in greater oxidation. Therefore, for Mo films deposited at high substrate inclination angles, patterns shown in Fig. 4 in terms of oxygen content progression might attest to a higher porosity percentage and consequently a reduced film density. The larger void fraction revealed by SEM measurements (Fig. 1) and the observation of a sharper increase in the oxygen content from $\alpha > 40°$ sound reasonably consistent.

### 3.3 Electrical resistivity

The evolution of Mo thin films electrical resistivity measured at room temperature *vs*. substrate inclination angle is shown in Fig. 5.

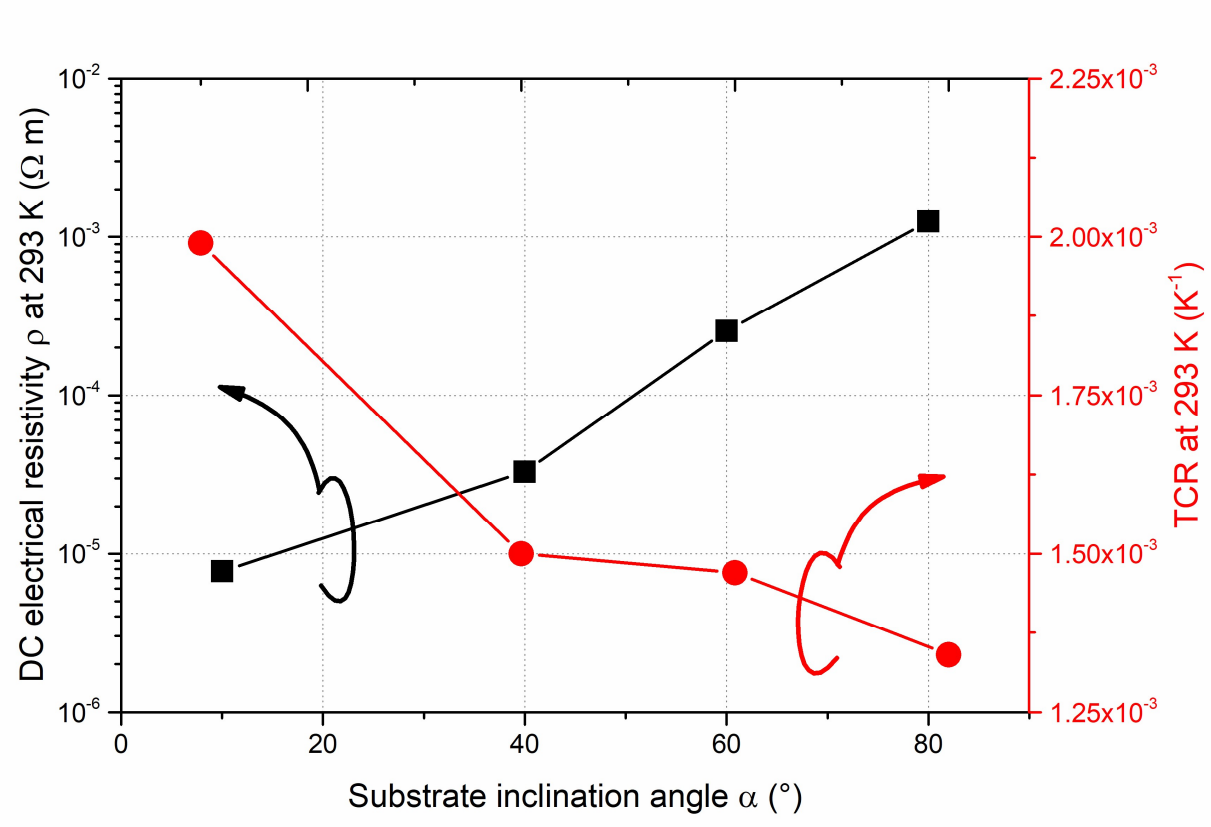

**Fig. 5.** DC electrical resistivity (ρ) and temperature coefficient of resistance (TCR) both determined at room temperature as a function of the substrate inclination angle of Mo thin films.

Changes of the film microstructure and chemical composition with substrate deposition angle also manifest themselves by variations in the room temperature electrical resistivity at least 2 orders of magnitude. DC electrical resistivity measured at room temperature increases from $\rho = 7.71\times10^{-6}$ to $1.25\times10^{-3}$ Ω m when α changes from 10 to 80 °, respectively. These values are several orders of magnitude higher than that of bulk Mo ($\rho_{Mo}$ bulk = $5.47\times10^{-8}$ Ω m at room temperature) [40]. This is mainly assigned to the high porosity typically produced in OAD thin films, especially using glancing substrate inclination angles. The electron scattering phenomenon becomes more important due to the increased presence of voids [47–49], and a reduction of the crystal size as illustrated from GIXRD results in Fig. 3b. They both contribute to reduce the electron mean free path of free electrons. In addition, the oxygen concentration becomes significant, as the substrate inclination angle is higher than 40° (Fig. 4). An amorphous oxide compound is formed between the tilted columns, which also prevents conduction paths of the free carriers. Similarly, the temperature coefficient of resistance (TCR) calculated from measurements of DC electrical resistivity as a function of the temperature from 20 to 100°C (not shown here) is also influenced by the substrate inclination angle (Fig. 5). It gradually drops from $1.99\times10^{-3}$ to $1.34\times10^{-3}$ $K^{-1}$ as the substrate inclination angle rises from 10 to 80°. These values are all significantly lower than that of the Mo bulk (for Mo bulk at room temperature, TCR = $4.53\times10^{-3}$ $K^{-1}$), as expected for thin films. However, tilting the substrate reduces the crystal size, as previously shown from XRD results (Fig. 3). In addition, an oxygen enrichment has been brought to the fore from analyses of the chemical composition (Fig. 4). An amorphization of the Mo films is then produced as α angle increases Assuming Reiss *et al.* investigations [50], this decrease of TCR *vs.* substrate inclination angle can be mainly assigned to the increasing number of grain boundaries per electron mean free path. Since high substrate inclination angles reduces the crystal size, electron scattering at grain boundaries is favored. Films become more resistive and a lower TCR, which may even exhibit a negative value although films remain in a conductive regime.

### 3.4 Wettability and SFE of OAD films

Contact angle measurements were carried out to analyze the wetting behavior of the Mo thin films. Mo films deposited at $\alpha = 10°$ were chosen as a reference (no tilted columns) and compared to the films deposited at $\alpha = 80°$. In Fig. 6, SEM top views of all films are shown as well as the corresponding optical micrographs of water droplets in contact with Mo surfaces.

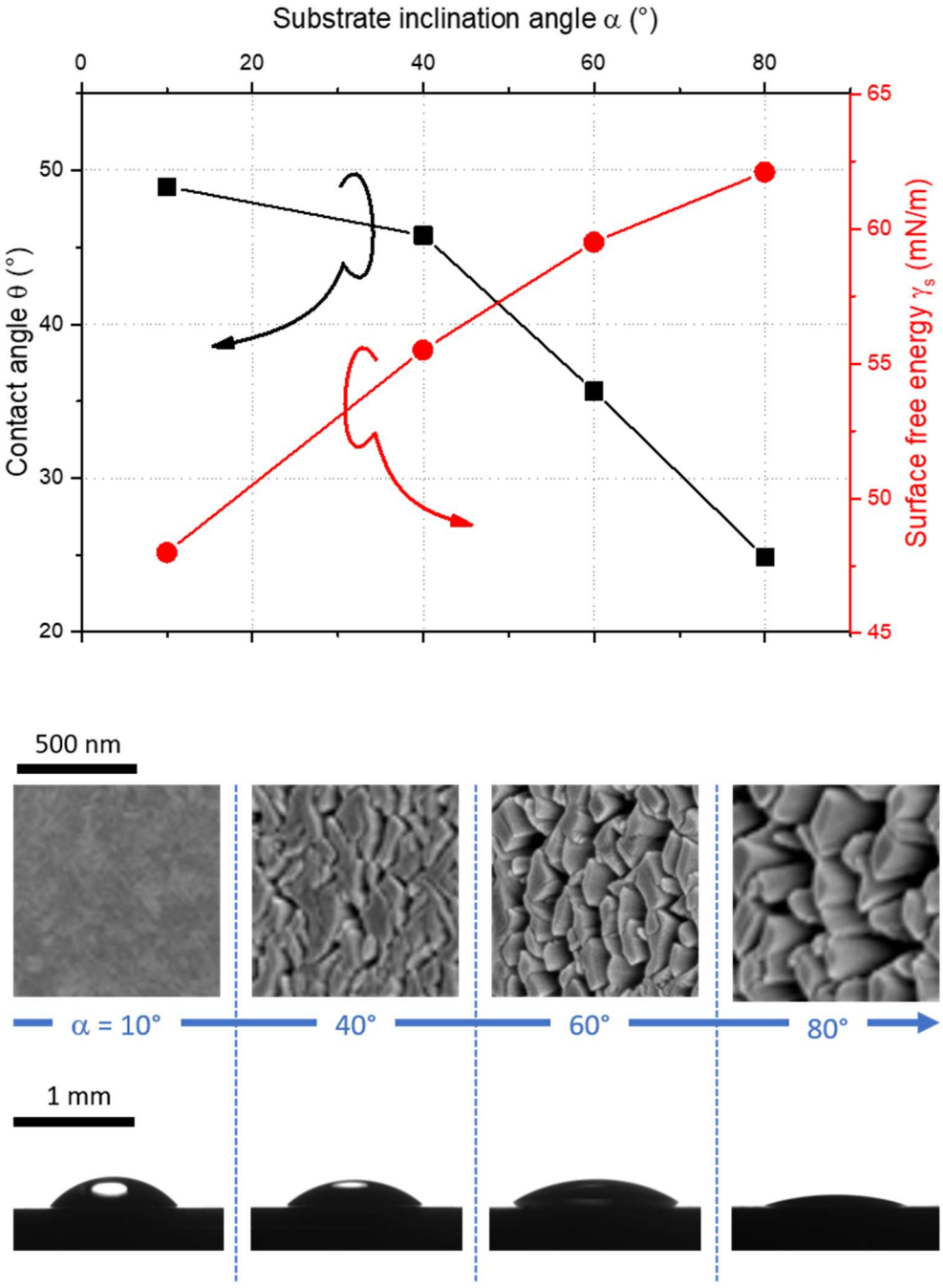


**Fig. 6.** Contact angle θ measured with distilled water and surface free energy $\gamma_s$ *vs.* substrate inclination angle α. Optical micrographs of water droplets in contact with Mo films and SEM top-view are given for each substrate inclination angle.

Usually, while measuring the contact angle, the liquid droplet spreads evenly in all directions over the solid surface. The main factors controlling the contact angle of liquid droplets on a solid are the chemistry and the roughness of the surface, which are intimately linked to the microstructure of the material [25, 51–54]. OAD techniques have been used to control the wettability of materials [21, 55, 56], as they allow precise control of both the surface chemistry and roughness. The development of a suitable surface texture is necessary to achieve either hydrophobicity or hydrophilicity. The contact angle decreases with increasing surface roughness and also for thin films exhibiting interconnected pores [57]. It was observed that the contact angle shows a direct correlation with the surface roughness of the thin films, and the model proposed by Wenzel can be applied.

The thin films' hydrophilic properties become stronger when substrate inclination angle increases, as shown from optical micrographs in Fig. 6. Based on the surface morphology and texture of the thin films, this could be expected. The contact angle of a surface depends on the size of the surface texture as well as the contact area between the drop and the surface. Two models can be used to understand the phenomenon of surface wetting on rough surfaces. The first model is that of Cassie-Baxter (applicable to hetero-structured materials with porous nanostructures) [58] and the second one from Wenzel (applicable to rough surfaces) [59–61]. However, Wenzel and Cassie-Baxter mixed states are frequently implemented because of the partial liquid penetration of the air pockets generated into the rough surface features. On the other hand, the impregnation state refers to a different state in the Wenzel region. Although it is outside the purview of this study, more information about this state's potential benefits for impregnated membranes can be found elsewhere [59–61]. For the mixed Wenzel-Cassie-Baxter and impregnation wetting states, the following equations can be used [62]. It is also essential to consider the morphology of the Mo thin films obtained in Fig. 1, which favors the mixed states because of the presence of porosity at high substrate inclination angle. The relationship between surface roughness and contact angle is described by Wenzel's equation:

$$\cos(\varepsilon_w) = r.cos(\varepsilon_Y) \quad (1)$$

where $r$ is the ratio of actual surface area to the geometric surface area (Arb. Units), $\varepsilon_w$ is the apparent contact angle (°), and $\varepsilon_Y$ is Young's contact angle (°).

A larger contact angle θ generally reflects a lower free surface energy. An important parameter to clarify the interfacial interaction of a solid surface with a contacting medium is the surface-free energy. For solids, this concept is typically stated as surface-free energy, and for liquids as interfacial tension. The surface hydrophilicity of a solid surface can be measured using two factors: The solid surface free energy of cohesion and the solid-water free energy of

adhesion. The free surface energy $\gamma_s$ of the films is determined from the contact angle θ measurements according to the OWRK model [24] (Owen, Wendt, Rabel, Kaelble) and is presented in Fig. 6. In this approach, Young's equation is modified to incorporate the dispersive and polar components of the surface free energy, according to:

$$\left(1 + cos(\theta)\right) = 2\sqrt{\gamma_s^p \ \gamma_L^p} + 2\sqrt{\gamma_s^d \ \gamma_L^d} \quad (2)$$

where $\gamma_S^p$, $\gamma_L^p$, $\gamma_S^d$ and $\gamma_L^d$ are the polar and dispersive parts of the solid and liquid surface energies, respectively. There is a significant increase of surface free energy for films deposited at $\alpha = 80°$ compared to those prepared with $\alpha = 10°$: $\gamma_s = 62\pm1$ and $48.0\pm2.2$ mN $m^{-1}$, respectively. It can be concluded that the wettability is significantly improved for OAD Mo thin films. An increase in surface roughness will provide a greater surface area for liquid contact. This requires a more appropriate analysis, taking into account the topography of the surface at the nanometric scale [63]. Thin films with a low polar component and a reasonably low surface free energy would exhibit high adhesion resistance, according to Lugscheider and Bobzin [64]. The current results show that Mo thin films is a favorable coating for tribological applications [65] and corrosion resistance when applied to reference films developed with a near-normal incidence by conventional sputtering.

## 4. Conclusion

Composition, crystalline structure, and morphology of 800 nm thick Mo thin films sputter-deposited by oblique angle deposition (OAD) are examined assuming the influence of the substrate inclination angle α. The potential for tailoring these films' responses by altering growth design and structural aspects are discussed.

The findings of this study illustrate that:

i) By changing the geometry of the growing films, it is possible to adjust the surface properties of Mo thin films, which is explained through the surface topography.

ii) Compared to samples prepared by conventional sputtering (normal incidence angle) with different compositions and crystalline phases, inclined geometries cause electrical characteristics to vary with a significant greater amplitude, i.e., more than 2 orders of magnitude. The increased post-growth oxidation of Mo films caused by rising inter-columnar film porosity at high angles was thought to be the cause of the

electrical resistivity increase as a function of the substrate deposition angle, with this effect being more prominent at higher angles ($\alpha = 80°$).

iii) Mo thin films prepared with $\alpha = 10°$ and 80° exhibit a contact angle of 50.5°and 28.7°, and a surface energy of 48.1 and 62.1 mN $m^{-1}$, respectively. The contact angle of all prepared samples showed a low value compared with dense Mo films because of the porous structure induced by the shadowing effect during the growth. The OAD technique also played a crucial role in the atomic and chemical compositions at the nanocolumnar film surface, which is considered to be one of the factors that affect the wettability properties. As a result, the highest substrate inclination angle produces a significant enhanced wettability, which makes it possible to control the surface wettability of architected OAD monolayers.

iv) These results highlight the prospect of modifying a thin film's response by modifying its design, which in turn affects its morphological and structural characteristics. They also pave the way for novel high-tech materials and emphasize the prospect of modifying a thin film's response by tuning its architecture. The latter strongly affects its morphological and structural characteristics, creating original nanostructured surfaces.

## Acknowledgement

This work has been supported by the Region Bourgogne Franche-Comté and by EIPHI Graduate School (Contract 'ANR-17-EURE-0002').

**CRediT authorship contribution statement**

Khaoula Rahmouni: Conceptualization; Investigation; Methodology; Writing – original draft . Ilyas Bensalem: Data curation;Formal Analysis. Abdelhamid Benhaya: Data curation;Formal Analysis. Nicolas Martin: Investigation; Methodology; Validation; Writing-rewiew & editing.

All authors have read and agreed to the published version of the manuscript.

**Declaration of interests**

The authors declare that they have no known competing financial interests or personal relationships that could have appeared to influence the work reported in this paper.

## References


[1] K. Inzani, M. Nematollahi, F. Vullum-Bruer, T. Grande, T.W. Reenaas, S.M. Selbach, Electronic properties of reduced molybdenum oxides, Phys. Chem. Chem. Phys. 19 (2017) 9232–9245. https://doi.org/10.1039/C7CP00644F.

[2] S. Min Lee, E. Hyun Kim, S. Man Koo, Synthesis and characterization of volatile liquid Mo precursors for vapor phase deposition of thin films containing molybdenum, Polyhedron. 240 (2023) 116445. https://doi.org/10.1016/j.poly.2023.116445.

[3] A.M. Taurino, A. Forleo, L. Francioso, P. Siciliano, M. Stalder, R. Nesper, Synthesis, electrical characterization, and gas sensing properties of molybdenum oxide nanorods, Appl. Phys. Lett. 88 (2006) 152111. https://doi.org/10.1063/1.2192571.

[4] M. Guo, B. Yuan, Y. Sui, Y. Xiao, J. Dong, L. Yang, L. Bai, H. Yang, D. Wei, W. Wang, H. Chen, Rational design of molybdenum sulfide/tungsten oxide solar absorber with enhanced photocatalytic degradation toward dye wastewater purification, J. Colloid Interface Sci. 631 (2023) 33–43. https://doi.org/10.1016/j.jcis.2022.11.015.

[5] Y. Tian, F. Li, Y. Song, J. Liu, J. Ji, F. Wang, Molybdenum nitride as a metallic photoelectrocatalyst for hydrogen evolution reaction via introduction of electron traps to improve the separation efficiency of photogenerated carriers, Int. J. Hydrog. Energy. 47 (2022) 10573–10582. https://doi.org/10.1016/j.ijhydene.2021.08.188.

[6] C. Caro, K. Thirunavukkarasu, M. Anilkumar, N.R. Shiju, G. Rothenberg, Selective Autooxidation of Ethanol over Titania-Supported Molybdenum Oxide Catalysts: Structure and Reactivity, Adv. Synth. Catal. 354 (2012) 1327–1336. https://doi.org/10.1002/adsc.201000841.

[7] J.B. Goodenough, Metallic oxides, Prog. Solid State Chem. 5 (1971) 145–399. https://doi.org/10.1016/0079-6786(71)90018-5.

[8] C. Martella, P. Melloni, E. Cinquanta, E. Cianci, M. Alia, M. Longo, A. Lamperti, S. Vangelista, M. Fanciulli, A. Molle, Engineering the Growth of MoS2 via Atomic Layer Deposition of Molybdenum Oxide Film Precursor, Adv. Electron. Mater. 2 (2016) 1600330. https://doi.org/10.1002/aelm.201600330.

[9] P. Taheri, J. Wang, H. Xing, J.F. Destino, M.M. Arik, C. Zhao, K. Kang, B. Blizzard, L. Zhang, P. Zhao, S. Huang, S. Yang, F.V. Bright, J. Cerne, H. Zeng, Growth mechanism of largescale MoS2 monolayer by sulfurization of MoO3 film, Mater. Res. Express. 3 (2016) 075009. https://doi.org/10.1088/2053-1591/3/7/075009.

[10] D. Boing, A.J. de Oliveira, R.B. Schroeter, Limiting conditions for application of PVD (TiAlN) and CVD (TiCN/Al2O3/TiN) coated cemented carbide grades in the turning of

hardened steels, Wear. 416–417 (2018) 54–61. https://doi.org/10.1016/j.wear.2018.10.007.

[11] D.T. Quinto, Technology perspective on CVD and PVD coated metal-cutting tools, Int. J. Refract. Met. Hard Mater. 14 (1996) 7–20. https://doi.org/10.1016/0263-4368(96)83413-5.

[12] R.J. Santos, A. Chuvilin, E. Modin, S.P. Rodrigues, S. Carvalho, M.T. Vieira, Nanoporous thin films obtained by oblique angle deposition of aluminum on porous surfaces, Surf. Coat. Technol. 347 (2018) 350–357. https://doi.org/10.1016/j.surfcoat.2018.05.022.

[13] G.D. Magnuson, B.B. Meckel, P.A. Harkins, Etch Effects from Oblique-Incidence Ion Bombardment, J. Appl. Phys. 32 (2004) 369–374. https://doi.org/10.1063/1.1736013.

[14] A.G. Dirks, H.J. Leamy, Columnar microstructure in vapor-deposited thin films, Thin Solid Films. 47 (1977) 219–233. https://doi.org/10.1016/0040-6090(77)90037-2.

[15] A. Amassian, K. Kaminska, M. Suzuki, L. Martinu, K. Robbie, Onset of shadowing-dominated growth in glancing angle deposition, Appl. Phys. Lett. 91 (2007) 173114. https://doi.org/10.1063/1.2794420.

[16] L. González-García, J. Parra-Barranco, J.R. Sánchez-Valencia, A. Barranco, A. Borrás, A.R. González-Elipe, M.-C. García-Gutiérrez, J.J. Hernández, D.R. Rueda, T.A. Ezquerra, Correlation lengths, porosity and water adsorption in TiO2 thin films prepared by glancing angle deposition, Nanotechnology. 23 (2012) 205701. https://doi.org/10.1088/0957-4484/23/20/205701.

[17] J.G.V. Dijken, M.D. Fleischauer, M.J. Brett, Controlled nanostructuring of CuPc thin films via glancing angle deposition for idealized organic photovoltaic architectures, J. Mater. Chem. 21 (2011) 1013–1019. https://doi.org/10.1039/C0JM03026K.

[18] H. Savaloni, F. Babaei, S. Song, F. Placido, Characteristics of sculptured Cu thin films and their optical properties as a function of deposition rate, Appl. Surf. Sci. 255 (2009) 8041–8047. https://doi.org/10.1016/j.apsusc.2009.05.011.

[19] R. Alvarez, J.M. García-Martín, M. Macías-Montero, L. Gonzalez-Garcia, J.C. González, V. Rico, J. Perlich, J. Cotrino, A.R. González-Elipe, A. Palmero, Growth regimes of porous gold thin films deposited by magnetron sputtering at oblique incidence: from compact to columnar microstructures, Nanotechnology. 24 (2013) 045604. https://doi.org/10.1088/0957-4484/24/4/045604.

[20] D. Toledano, R.E. Galindo, M. Yuste, J.M. Albella, O. Sánchez, Compositional and structural properties of nanostructured ZnO thin films grown by oblique angle reactive

sputtering deposition: effect on the refractive index, J. Phys. Appl. Phys. 46 (2012) 045306. https://doi.org/10.1088/0022-3727/46/4/045306.

[21] A. Barranco, A. Borras, A.R. Gonzalez-Elipe, A. Palmero, Perspectives on oblique angle deposition of thin films: From fundamentals to devices, Prog. Mater. Sci. 76 (2016) 59–153. https://doi.org/10.1016/j.pmatsci.2015.06.003.

[22] O. Philips'Gloeilampenfabrieken, A method of measuring specific resistivity and Hall effect of discs of arbitrary shape, Philips Res Rep. 13 (1958) 1–9.

[23] V. Pachchigar, B.K. Parida, S. Augustine, S. Hans, M. Saini, K.P. Sooraj, M. Ranjan, Comparative wettability study of bulk and thin film of polytetrafluoroethylene after low energy ion irradiation, Thin Solid Films. 777 (2023) 139888. https://doi.org/10.1016/j.tsf.2023.139888.

[24] R. Mareus, C. Mastail, F. Anğay, N. Brunetière, G. Abadias, Study of columnar growth, texture development and wettability of reactively sputter-deposited TiN, ZrN and HfN thin films at glancing angle incidence, Surf. Coat. Technol. 399 (2020) 126130. https://doi.org/10.1016/j.surfcoat.2020.126130.

[25] M.F. Ismail, B. Khorshidi, M. Sadrzadeh, New insights into the impact of nanoscale surface heterogeneity on the wettability of polymeric membranes, J. Membr. Sci. 590 (2019) 117270. https://doi.org/10.1016/j.memsci.2019.117270.

[26] R. Alvarez, C. Lopez-Santos, J. Parra-Barranco, V. Rico, A. Barranco, J. Cotrino, A.R. Gonzalez-Elipe, A. Palmero, Nanocolumnar growth of thin films deposited at oblique angles: Beyond the tangent rule, J. Vac. Sci. Technol. B. 32 (2014) 041802. https://doi.org/10.1116/1.4882877.

[27] R.N. Tait, T. Smy, M.J. Brett, A ballistic deposition model for films evaporated over topography, Thin Solid Films. 187 (1990) 375–384. https://doi.org/10.1016/0040-6090(90)90058-L.

[28] M.M. Hawkeye, M.J. Brett, Glancing angle deposition: Fabrication, properties, and applications of micro- and nanostructured thin films, J. Vac. Sci. Technol. A. 25 (2007) 1317–1335. https://doi.org/10.1116/1.2764082.

[29] R.N. Tait, T. Smy, M.J. Brett, Modelling and characterization of columnar growth in evaporated films, Thin Solid Films. 226 (1993) 196–201. https://doi.org/10.1016/0040-6090(93)90378-3.

[30] A. Siad, A. Besnard, C. Nouveau, P. Jacquet, Critical angles in DC magnetron glad thin films, Vacuum. 131 (2016) 305–311. https://doi.org/10.1016/j.vacuum.2016.07.012.

[31] Y. Zhao, Y. He, C. Brown, Composition dependent nanocolumn tilting angle during the oblique angle co-deposition, Appl. Phys. Lett. 100 (2012) 033106. https://doi.org/10.1063/1.3676665.

[32] H. Zhu, W. Cao, G.K. Larsen, R. Toole, Y. Zhao, Tilting angle of nanocolumnar films fabricated by oblique angle deposition, J. Vac. Sci. Technol. B. 30 (2012) 030606. https://doi.org/10.1116/1.4710999.

[33] R. El Beainou, N. Martin, V. Potin, P. Pedrosa, M.A.P. Yazdi, A. Billard, Correlation between structure and electrical resistivity of W-Cu thin films prepared by GLAD co-sputtering, Surf. Coat. Technol. 313 (2017) 1–7. https://doi.org/10.1016/j.surfcoat.2017.01.039.

[34] P. Pedrosa, A. Ferreira, N. Martin, M.A.P. Yazdi, A. Billard, S. Lanceros-Méndez, F. Vaz, Nano-sculptured Janus-like TiAg thin films obliquely deposited by GLAD co-sputtering for temperature sensing, Nanotechnology. 29 (2018) 355706. https://doi.org/10.1088/1361-6528/aacba8.

[35] H. Ferhati, F. Djeffal, N. Martin, Highly improved responsivity of self-powered UV–Visible photodetector based on TiO2/Ag/TiO2 multilayer deposited by GLAD technique: Effects of oriented columns and nano-sculptured surface, Appl. Surf. Sci. 529 (2020) 147069. https://doi.org/10.1016/j.apsusc.2020.147069.

[36] R. El Beainou, N. Martin, V. Potin, P. Pedrosa, M.A.P. Yazdi, A. Billard, W-Cu sputtered thin films grown at oblique angles from two sources: Pressure and shielding effects, Surf. Coat. Technol. 343 (2018) 153–159. https://doi.org/10.1016/j.surfcoat.2017.09.062.

[37] J. Wei, P. Guo, L. Liu, H. Li, H. Li, S. Wang, P. Ke, A. Wang, Tailored electrochemical behavior of ta-C film by glancing angle deposition, Appl. Surf. Sci. 516 (2020) 146115. https://doi.org/10.1016/j.apsusc.2020.146115.

[38] K. Rahmouni, A. Besnard, K. Oulmi, C. Nouveau, A. Hidoussi, L. Aissani, M. Zaabat, In vitro corrosion response of CoCrMo and Ti-6Al-4V orthopedic implants with Zr columnar thin films, Surf. Coat. Technol. 436 (2022) 128310. https://doi.org/10.1016/j.surfcoat.2022.128310.

[39] D.J. Poxson, F.W. Mont, M.F. Schubert, J.K. Kim, E.F. Schubert, Quantification of porosity and deposition rate of nanoporous films grown by oblique-angle deposition, Appl. Phys. Lett. 93 (2008) 101914. https://doi.org/0003-6951/2008/93(10))101914/3/$23/00.

[40] D.R. Lide, CRC Handbook of Chemistry and Physics, 85th Edition, CRC Press, 2004.

[41] G. Abadias, F. Anğay, R. Mareus, C. Mastail, Texture and Stress Evolution in HfN Films Sputter-Deposited at Oblique Angles, Coatings. 9 (2019) 712. https://doi.org/10.3390/coatings9110712.

[42] F.V. Grigoriev, V.B. Sulimov, A.V. Tikhonravov, Stress distribution in highly porous SiO2 films: Results of the molecular dynamics simulation, IOP Conf. Series: Mater. Sci. Eng. 904 (2020) 012004. https://doi.org/10.1088/1757-899X/904/1/012004.

[43] B. Bouaouina, C. Mastail, A. Besnard, R. Mareus, F. Nita, A. Michel, G. Abadias, Nanocolumnar TiN thin film growth by oblique angle sputter-deposition: Experiments vs. simulations, Mater. Des. 160 (2018) 338–349. https://doi.org/10.1016/j.matdes.2018.09.023.

[44] C. Oros, C. Chananonnawathorn, W. Hincheeranan, C. Jetjamnong, T. Chaikeeree, N. Wongdamnern, M. Horprathum, Optical and structural properties of WO3 nanostructure films prepared by oblique angle deposition, Mater. Today Proc. 65 (2022) 2322–2326. https://doi.org/10.1016/j.matpr.2022.05.216.

[45] W. Phae-ngam, M. Horprathum, C. Chananonnawathorn, T. Lertvanithphol, B. Samransuksamer, P. Songsiriritthigul, H. Nakajima, S. Chaiyakun, Oblique angle deposition of nanocolumnar TiZrN films via reactive magnetron co-sputtering technique: The influence of the Zr target powers, Curr. Appl. Phys. 19 (2019) 894–901. https://doi.org/10.1016/j.cap.2019.05.002.

[46] P. Pokorný, J. Musil, P. Fitl, M. Novotný, J. Lančok, J. Bulíř, Contamination of Magnetron Sputtered Metallic Films by Oxygen From Residual Atmosphere in Deposition Chamber, Plasma Process. Polym. 12 (2015) 416–421. https://doi.org/10.1002/ppap.201400172.

[47] A. Besnard, N. Martin, C. Millot, J. Gavoille, R. Salut, Effect of sputtering pressure on some properties of chromium thin films obliquely deposited, IOP Conf. Ser. Mater. Sci. Eng. 12 (2010) 012015. https://doi.org/10.1088/1757-899X/12/1/012015.

[48] H. Boukhalfa, V. Potin, N. Martin, Structural and electrical properties of nanocolumnar W-Mo thin films with a Janus-like structure, Surf. Coat. Technol. 448 (2022) 128928. https://doi.org/10.1016/j.surfcoat.2022.128928.

[49] F.G. Cougnon, I.C. Schramm, D. Depla, On the electrical properties of sputter deposited thin films: The role of energy and impurity flux, Thin Solid Films. 690 (2019) 137540. https://doi.org/10.1016/j.tsf.2019.137540.

[50] G. Reiss, J. Vancea, H. Hoffmann, Grain-boundary resistance in polycrystalline metals. Phys. Rev. Lett. 56 (1986) 2100. https://doi.org/10.1103/PhysRevLett.56.2100.

[51] D. Magnfält, G. Abadias, K. Sarakinos, Atom insertion into grain boundaries and stress generation in physically vapor deposited films, Appl. Phys. Lett. 103 (2013) 051910. https://doi.org/10.1063/1.4817669.

[52] R. Blossey, Self-cleaning surfaces — virtual realities, Nat. Mater. 2 (2003) 301–306. https://doi.org/10.1038/nmat856.

[53] L. D'Avico, R. Beltrami, E. Pargoletti, S.P.M. Trasatti, G. Cappelletti, Insight into the Release Agents/PVD Coatings Interaction for Plastic Mold Technology, Coatings. 10 (2020) 281. https://doi.org/10.3390/coatings10030281.

[54] B. Abdallah, M. Naddaf, M. A-Kharroub, Structural, mechanical, electrical and wetting properties of ZrNx films deposited by Ar/N2 vacuum arc discharge: Effect of nitrogen partial pressure, Nucl. Instrum. Methods Phys. Res. Sect. B Beam Interact. Mater. At. 298 (2013) 55–60. https://doi.org/10.1016/j.nimb.2013.01.003.

[55] A. Bayat, M. Ebrahimi, A.Z. Moshfegh, Correlation between surface roughness and hydrophobicity of GLAD RF sputtered PTFE/W/Glass nanorod thin films, Vacuum. 101 (2014) 279–282. https://doi.org/10.1016/j.vacuum.2013.09.007.

[56] Y. Rahmawan, H. Yoon, M.-W. Moon, H.-G. Jeong, K.-Y. Suh, Janus-faced micro and nanopillars for geometry and surface chemistry controllable bioinspired dry adhesives, J. Adhes. Sci. Technol. 28 (2014) 367–386. https://doi.org/10.1080/01694243.2012.693825.

[57] B. Xiong, J. Li, C. He, X. Tang, Z. Lv, X. Li, X. Yan, Effect of morphology and surface roughness on wettability of porous titania films, Mater. Res. Express 7 (2020) 115013. https://doi.org/10.1088/2053-1591/abc770.

[58] Y. Jiang, Z. Yang, T. Jiang, D. Shen, J. Duan, Banana Leaf Surface's Janus Wettability Transition from the Wenzel State to Cassie–Baxter State and the Underlying Mechanism, Materials. 15 (2022) 917. https://doi.org/10.3390/ma15030917.

[59] F. Liu, B. Yi, D. Xing, J. Yu, H. Zhang, Nafion/PTFE composite membranes for fuel cell applications, J. Membr. Sci. 212 (2003) 213–223. https://doi.org/10.1016/S0376-7388(02)00503-3.

[60] M.H. Yildirim, D. Stamatialis, M. Wessling, Dimensionally stable Nafion–polyethylene composite membranes for direct methanol fuel cell applications, J. Membr. Sci. 321 (2008) 364–372. https://doi.org/10.1016/j.memsci.2008.05.013.

[61] M.F. Macgam, B. Khorshidi, A. Tehrani-Bagha, M. Sadrzadeh, Surface characterization of thin-film composite membranes using contact angle technique: Review of quantification strategies and applications, Adv. Colloid Interface Sci. 299 (2022) 102524. https://doi.org/10.1016/j.cis.2021.102524.

[62] M.N. MacGregor-Ramiasa, K. Vasilev, Questions and Answers on the Wettability of Nano-Engineered Surfaces, Adv. Mater. Interfaces. 4 (2017) 1700381. https://doi.org/10.1002/admi.201700381.

[63] K.V. Chauhan, N.P. Patel, D. Subhedar, Z. Sonara, A.S. Thakkar, Influence of nitrogen environment on wettability and optical properties of sputtered zirconium nitride thin film, Mater. Today Proc. (2023). https://doi.org/10.1016/j.matpr.2023.08.218.

[64] E. Lugscheider, K. Bobzin, The influence on surface free energy of PVD-coatings, Surf. Coat. Technol. 142-144 (2001) 755-760. https://doi.org/10.1016/S0257-8972(01)01315-9.

[65] N.J. Hallab, K.J. Bundy, K. O'Connor, R. Clark, R.L. Moses, Cell adhesion to biomaterials: correlations between surface charge, surface roughness, adsorbed protein, and cell morphology, J. Long. Term Eff. Med. Implants. 5 (1995) 209–231.